***JKPK (JURNAL KIMIA DAN PENDIDIKAN KIMIA)**, Vol. 10, No. 2, 2025* *pp. 462-476*
*Chemistry Education Study Program, Universitas Sebelas Maret* *ISSN 2503-4146*
*https://jurnal.uns.ac.id/jkpk* *ISSN 2503-4154 (online)*

# Chitosan-Silica (CS/Sc) Composites as Promising Adsorbents for Fe(III) Removal in Water Purification

**Yulida Amri[1*], Fakhira Khairana[1], Ida Ratna Nila[2], Rahmatul Fajri[1]**

*[1]Department of Chemistry, Faculty of Science and Technology, Universitas Samudra Kota Langsa, Aceh, Indonesia*
*[2]Department of Physics, Faculty of Science and Technology, Universitas Samudra, Kota Langsa, Aceh, Indonesia*

## ABSTRACT

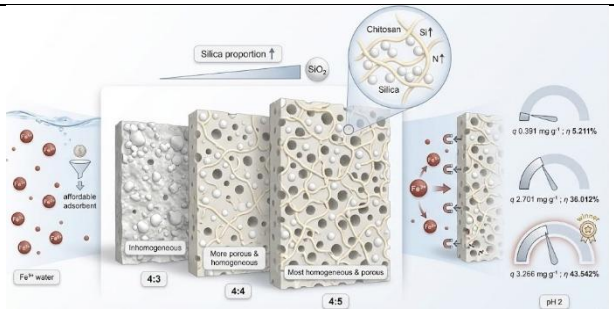


Fe(III) contaminated water has become a serious environmental concern, creating a need for effective and affordable adsorbents. This study evaluates the performance of chitosan silica (CS/Sc) composites for Fe(III) removal. CS/Sc composites were synthesized via a sol-gel route by varying the volume ratio of 1% chitosan to 5% silica. The ratio significantly influenced surface morphology. The 4:3 composition showed silica dominance with an inhomogeneous surface, while the 4:4 composition exhibited a more porous and homogeneous structure. The 4:5 composition yielded the most homogeneous and porous surface, exhibiting increased Si and N signals, which indicate a stronger interaction between chitosan and silica. Fe(III) adsorption tests were conducted at pH 2. Both adsorption capacity (q) and adsorption efficiency (η) increased with increasing silica proportion. The CS/Sc 4:3 composite showed an adsorption capacity q of 0.391 mg $g^{-1}$ and an adsorption efficiency η of 5.211%. The 4:4 composite reached q of 2.701 mg $g^{-1}$ and η of 36.012%. The highest performance was obtained with the 4:5 composite, yielding a q of 3.266 mg $g^{-1}$ and an η of 43.542%. These results demonstrate that the CS/Sc composite with a 4:5 ratio is the most promising formulation for Fe(III) removal and water purification applications. The novelty of this work lies in the targeted application of CS/Sc composites for Fe(III) adsorption, which has been rarely reported, and in providing insight into how compositional variation affects structure and adsorption performance.

**Keywords:** *Composite; Chitosan; Silica; Fe(III); Adsorbent.*
**Corresponding Author: yulidaamri@unsam.ac.id*
**How to cite:** Y. Amri, F. Khairana, I.R. Nila, and R. Fajri, "Chitosan-Silica (CS/Sc) Composites as Promising Adsorbents for Fe(III) Removal in Water Purification," *Jurnal Kimia dan Pendidikan Kimia (JKPK)*, vol. 10, no. 3, pp.462-476, 2025. [Online]. Available: https://doi.org/10.20961/jkpk.v10i3.107769
***Received:*** *2025-08-07* ***Accepted:*** *2025-12-21* ***Published:*** *2025-12-31*

## INTRODUCTION

Heavy metal contamination in water bodies is a major global environmental problem. Industrial effluents, mining activities, agricultural runoff, and domestic waste all contribute to the release of heavy metals into aquatic systems. Because heavy metals are toxic, non-biodegradable, and prone to bioaccumulation, their presence in water poses serious risks to ecosystems and human health [1].

Several metals, such as iron (Fe), cadmium (Cd), and lead (Pb), can degrade water quality [2]. These contaminants may enter the human body through contaminated food and drinking water. Iron is an essential

micronutrient that supports metabolic processes; however, excessive exposure can lead to toxicity [3]. High iron concentrations can increase cancer risk by forming hydroxyl radicals (•OH), which induce oxidative stress and damage DNA structures [4]. The World Health Organization sets the permissible concentration of iron in drinking water at 0.3 ppm [5].

One practical approach to reduce heavy metal levels is adsorption using materials with high adsorption capacity (q). Common adsorbents used in wastewater treatment include activated carbon [6], chitosan [7], metal-organic frameworks (MOFs) [8], bentonite [9], silica [10], and nanotube-based materials [11]. Activated carbon is effective but often costly, with limited selectivity and relatively poor mechanical stability. MOFs offer high surface area and tunable functionality, yet their synthesis can be complex and expensive. In addition, many MOFs exhibit limited chemical and mechanical stability, face challenges in large-scale production, and may show inconsistent performance under practical operating conditions [12].

Chitosan is a natural biopolymer derived from the shells of crustaceans such as crabs and shrimp [13]. It has attracted considerable attention as a membrane and adsorbent material and can also function as a natural coagulant (bioagulant), making it suitable for environmentally friendly water treatment applications [14]. Chitosan is capable of removing organic pollutants through hydrogen bonding interactions, which explains its widespread use in water purification processes [15]. To further enhance its adsorption performance, chitosan can be combined with inorganic materials such as silica, resulting in composite adsorbents with higher adsorption capacity and improved structural stability [16].

Previous studies have reported the successful application of chitosan–silica (CS Sc) composites as adsorbents for heavy metals such as Cu, Pb, and Ni in aqueous systems, demonstrating their effectiveness in reducing metal concentrations [17]. Similar biopolymer-based composites, including chitosan–kaolin materials, have also shown high efficiency for Cu removal, further supporting the potential of chitosan-based adsorbents [18]. In addition, CS Sc composites have been successfully applied for the adsorption of anionic dyes, yielding favorable adsorption performance [16]. However, the use of CS Sc composites specifically for the adsorption of iron (Fe) has not been extensively investigated.

In this study, a CS Sc composite was synthesized and evaluated as an adsorbent for Fe(III) in water. The objective was to assess the effectiveness and adsorption capacity of the composite toward Fe(III). Adsorption performance was quantified using Atomic Absorption Spectrophotometry (AAS). At the same time, the synthesized composite was characterized using Fourier Transform Infrared Spectroscopy (FTIR) and Scanning Electron Microscopy coupled with Energy Dispersive X-ray analysis (SEM EDX).

## METHODS

### 1. Chemicals and Reagents

The materials used in this study were distilled water, filter paper (rough grade 58x58), chitosan (technical grade), sodium metasilicate ($Na_2SiO_3$) (technical grade), universal indicator (Merck), glacial acetic acid ($CH_3COOH$) (analytical grade, Sigma-Aldrich), nitric acid ($HNO_3$) (analytical grade, Sigma-Aldrich), hydrochloric acid (HCl) (analytical grade, Sigma-Aldrich), sodium hydroxide (NaOH) (analytical grade, Sigma-Aldrich), ferrous ammonium sulfate [$Fe(NH_4)_2(SO_4)_2$] (analytical grade, Sigma-Aldrich), concentrated sulfuric acid ($H_2SO_4$) (analytical grade, Sigma-Aldrich), and potassium permanganate ($KMnO_4$) (analytical grade, Merck).

**2. Instrumentation**

The tools used in this study were glassware, analytical balance (GR-200), hotplate stirrer (MS300HS), portable pH meter (ATC), universal oven (Memmert), Atomic Absorption Spectrophotometer (AAS Varian AA240FS), Fourier Transform Infrared Spectroscopy (The Cary 630 FTIR Spectrometer with ATR Sampling Module), and Scanning Electron Microscope-Energy Dispersive X-Ray (SEM-EDX ZEISS EVO MA 10).

**3. Preparation of 1% (w/v) Chitosan Solution**

Ten grams of chitosan were placed in a beaker, and then 1,000 mL of a 2% (v/v) acetic acid solution was added. The mixture was stirred until dissolved.

**4. Preparation of 5% (w/v) Silica Solution**

Fifty grams of sodium metasilicate were placed in a beaker, and 1000 mL of distilled water was added. The mixture was stirred until the silica dissolved.

**5. Preparation and Characterization of CS/Sc Composite**

CS/Sc composites were prepared using sodium metasilicate (as silica) with variation in the CS/Sc ratio to adsorb Fe(III). This procedure is a modification of the previously reported method [17][18][19]. Variations in the volume ratio of chitosan-silica were made, namely 4:3, 4:4, and 4:5, using 1% chitosan and 5% silica. A silica solution is added dropwise to the chitosan solution. The chitosan and silica solutions were mixed slowly while stirring for 80 minutes at room temperature.

The resulting CS/Sc composite was then washed with 1000 mL of distilled water to remove residual acid until neutral (pH=7). The resulting product was then dried at 50°C until it was completely dry. The obtained product was weighed and then characterized by FTIR to determine the presence of functional groups. Testing with SEM-EDX was conducted to examine the morphology of the CS/Sc composites.

**6. Preparation of Calibration Curve**

A Fe(III) 100 ppm stock solution was prepared. A total of 20 mL of concentrated H2SO4 was added to 50 mL of distilled water, and 0.702 grams of Fe(NH4)2(SO4)2 (analytical grade, Sigma-Aldrich) was weighed and dissolved. KMnO4 solution was added dropwise until a faint pink color was formed. Then, it was diluted with 500 mL of distilled water.

The stock solution of Fe(III) 100 ppm was diluted to concentrations of 0 ppm, 5 ppm, 10 ppm, 15 ppm, and 20 ppm. The absorbance of each solution was measured using AAS, and then a calibration curve was

made. Measurement with AAS using a Hollow Cathode Lamp (HCL), Fe at a wavelength of ~248.3 nm.

**7. Application of CS/Sc Composite as Fe(III) adsorbent**

500 mL of Fe(III) 15 ppm was measured, and the pH was adjusted to 2 by adding 0.1 M HCl and 0.1 M NaOH. Then, 50 mL of the pH 2 Fe(III) 15 ppm solution was pipetted, and 0.1 gram of the CS/Sc composite was added. Stirred for 80 minutes at 120 rpm, the mixture was filtered, and 3-5 drops of HNO3 were added to prevent precipitation of Fe(III) ions.

. The remaining Fe(III) concentration was then analyzed using AAS. The same procedure was repeated for CS/Sc composites produced at various volume ratios. Measurements with AAS were repeated 3 times for each composite ratio. Data were analyzed using ANOVA at a significance level of 0.05. The % adsorption efficiency (η) and the adsorption capacity (q) can be calculated, respectively, using the following equations [17]:

$$\%(\eta) = \frac{(C_i - C_f)}{C_i}\ x\ 100\% \quad (1)$$

$$q\ \left(\frac{mg}{g}\right) = \frac{C_i - C_f}{C_i}\ x\ v \quad (2)$$

Where Ci is the initial Fe(III) concentration (mg $L^{-1}$), Cf is the final Fe(III) concentration after adsorption (mg $L^{-1}$), w is the mass of the CS/Sc composite used (g), and v is the total volume of the Fe(III) solution (L).

## RESULT AND DISCUSSION

**1. In-situ Silica Network Formation in the Chitosan Matrix**

CS/Sc composite was synthesized using the sol-gel method, a wet chemical method commonly employed for the synthesis of various materials. This method is simple, low-cost, and uses low temperatures [20].

**Table 1.** CS/Sc composites synthesis at different volume ratios

| CS/Sc volume ratios | Initial pH of CS solution | Final pH after SC addition | Product weight (gram) |
|---|---|---|---|
| 4:3 | 3 | 7.2 | 4.90 |
| 4:4 | 3 | 9.6 | 2.08 |
| 4:5 | 3 | 10.8 | 1.71 |

Table 1 shows the synthesis of CS/Sc composites at different volume ratios. The addition of silica to chitosan dissolved in acetic acid (pH 3) causes an increase in pH. This is because sodium metasilicate produces silicate ions when dissolved in water, which can hydrolyze to produce $OH^-$ Ions. The more silica added, the higher the pH of the solution.

Sodium metasilicate is utilized as a cost-effective source of silica and a precursor for various applications. In the sol-gel method, silica undergoes hydrolysis under acidic conditions to form silanol groups (Si-OH bonds), followed by a condensation reaction that forms a Si-O-Si network [21]. The reaction can be seen in the following equation [22][23]:

$$\text{Hydrolysis: } Na_2SiO_3 + H_2O + CH_3COOH \longrightarrow Si{-}(OH)_4 + 2CH_3COONa \quad (1)$$

$$\text{Condensation: } Si{-}(OH)_4 + Si{-}(OH)_4 \longrightarrow (HO)_3{-}Si{-}O{-}Si{-}(OH)_3 + H_2O \quad (2)$$

The subsequent gelation process occurs through electrostatic interactions between the silanol (Si-OH) groups and the amino groups of chitosan. Hydrogen bonds also form between the silanol groups of silica, as well as amino, hydroxyl, and acetate groups. In short, physical and chemical interactions determine the formation of new composite materials. [24]. The formation of hydrogen bonds between the amino and hydroxyl groups of chitosan with silica shows that chitosan can be integrated with silica through non-covalent bonds. [25][26]. In addition, the results of other studies show that silanol groups can bind to chitosan through the formation of Si-O-C covalent bonds using 3-glycidoxypropyl trimethoxysilane (GPTMS) as a coupling (crosslinker) agent. [27][28][29].

## 2. Characterization of CS/Sc Composites Using FTIR

Fourier Transform Infrared (FTIR) analysis was conducted to confirm the formation of the CS/Sc composite. The spectra of pure chitosan, pure silica, and the CS/Sc composites were examined and compared to identify characteristic functional group changes that indicate interactions between the two components. The FTIR spectra of chitosan (CS), silica (Sc), and the CS/Sc composites are presented in Figure 1

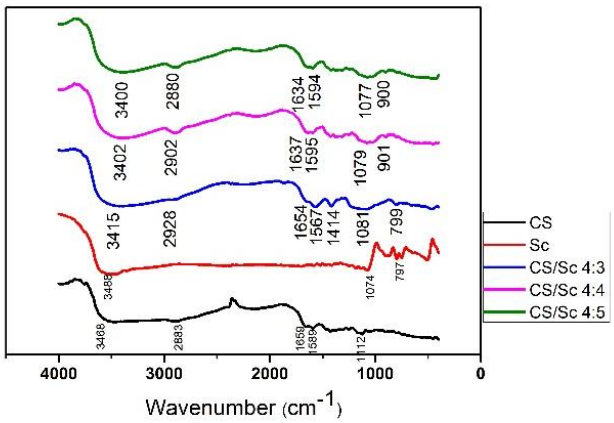


**Figure 1.** FTIR spectra of CS, Sc, CS/Sc 4:3, CS/Sc 4:4, and CS/Sc 4:5

The FTIR spectrum of chitosan shows a characteristic broad band at around 3468 $cm^{-1}$, which is attributed to overlapping O–H and N–H stretching vibrations from hydroxyl and amine groups. The band at 1659 $cm^{-1}$ corresponds to amide I (C=O stretching), while the band at 1589 $cm^{-1}$ is assigned to amide II (N–H bending). Additional bands at 1112 $cm^{-1}$, 1422 $cm^{-1}$, and 2883 $cm^{-1}$ are associated with C–O stretching, C–H bending, and C–H stretching vibrations, respectively [30].

The FTIR spectrum of silica displays a strong absorption band at 1074 $cm^{-1}$,

originating from asymmetric stretching vibrations of Si–O–Si bonds. A broad band near 3488 $cm^{-1}$ indicates O–H stretching from silanol groups and adsorbed water, while the band at 797 $cm^{-1}$ is attributed to Si–O vibrations [31][32].

The FTIR spectra of the CS/Sc composites combine features of both chitosan and silica, with several changes that indicate interaction between the two components. The broad band in the 3200–3500 $cm^{-1}$ region remains present in all composites but becomes broader and slightly shifted compared with pure chitosan, suggesting hydrogen bonding between chitosan (O–H and N–H) and silica (Si–OH) groups. The amide bands near 1659 $cm^{-1}$ and 1589 $cm^{-1}$ decrease in intensity and shift slightly, which is consistent with hydrogen bonding and possible electrostatic interactions involving chitosan amine or amide groups and silanol sites on silica [24][25][26][29]. This attenuation is most pronounced in the CS/Sc 4:5 sample, indicating stronger interaction at the higher silica ratio.

Bands in the 1070–1100 $cm^{-1}$ region appear in all composites, reflecting contributions from Si–O–Si and potentially Si–O–C linkages within the composite structure [23][29]. Broadening in this region further supports interactions between Si–O groups and the chitosan matrix. A strong band at around 799 $cm^{-1}$ is particularly evident in the CS/Sc 4:3 composite and is assigned to symmetric stretching or bending of Si–O–Si, indicating silica dominance in this composition [29][33]. Additional bands near 900 $cm^{-1}$ in the CS/Sc 4:4 and 4:5 composites can be attributed to silanol (Si–OH) groups, which may reflect increased surface hydroxylation and interaction sites [29][33][34]. Overall, the observed spectral shifts, band broadening, and intensity changes indicate that chitosan and silica interact through chemical and physicochemical interactions rather than forming a simple physical mixture. These FTIR results therefore support the successful formation of the CS/Sc composite with an integrated silica network within the chitosan matrix.

### 3. Characterization of CS/Sc Composites Using SEM-EDX

Chitosan–silica composites have been widely investigated because of their potential as adsorbents for environmental applications [24] and as functional materials in biomedical fields [35][36]. Pore structure is a key factor that influences adsorption efficiency because it governs surface area, accessibility of active sites, and mass transfer during adsorption [37][38]. Morphological characterization using SEM is therefore essential for the development of adsorbents. SEM, coupled with EDX, enables the visualization of surface features, including pore formation, and simultaneously provides elemental information that supports the interpretation of composite composition [39]. SEM observations reveal that the CS/Sc (4:3) composite exhibits a non-homogeneous surface morphology (Figure 2). The corresponding EDX results in Figure 5 indicate that this composite is primarily composed of Si. The surface appears relatively inhomogeneous, and distinct pores are not clearly observed. This morphology is

consistent with the low adsorption capacity (q) obtained for this composition, because limited pore development can restrict access to adsorption sites and reduce overall adsorption performance [40].

Figure 3 shows that the CS/Sc (4:4) composite exhibits a clear morphological improvement compared to the CS/Sc (4:3) composite. The surface appears more homogeneous, and initial pore features begin to emerge, indicating more favorable interactions between chitosan and silica. However, adsorption performance at this ratio remains relatively low, as reflected by the adsorption capacity (q) and adsorption efficiency (η) values in Table 2. A further improvement is observed in the CS/Sc (4:5) composite (Figure 4), which displays a finer, more uniform surface and more visible pore structures. The presence of pores is important because it increases accessibility to active sites and generally supports higher adsorption capacity [38].

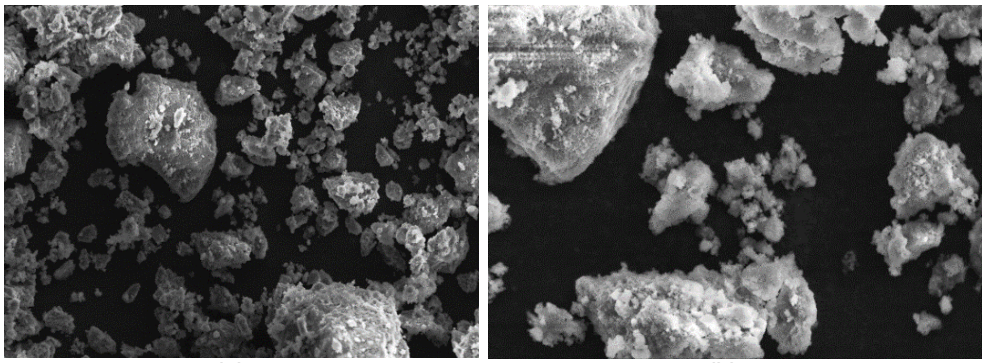

(a) (b)

**Figure 2.** SEM results of CS/Sc composite (4:3) (a) magnification 500X (b) magnification 1500X

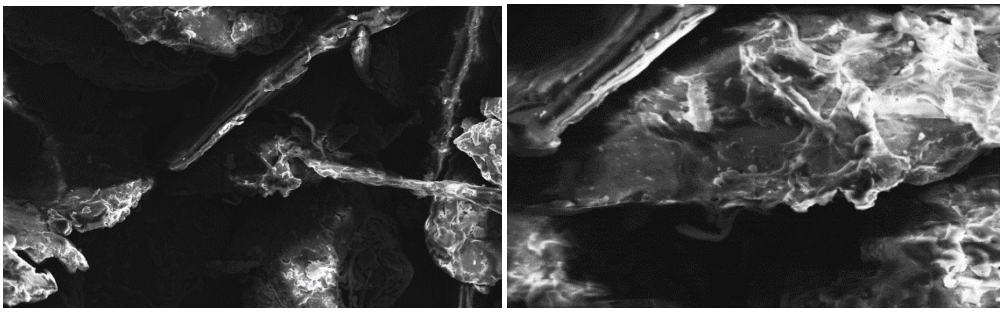

(a) (b)

**Figure 3.** SEM results of CS/Sc composite (4:4) (a) magnification 500X (b) magnification 1500X

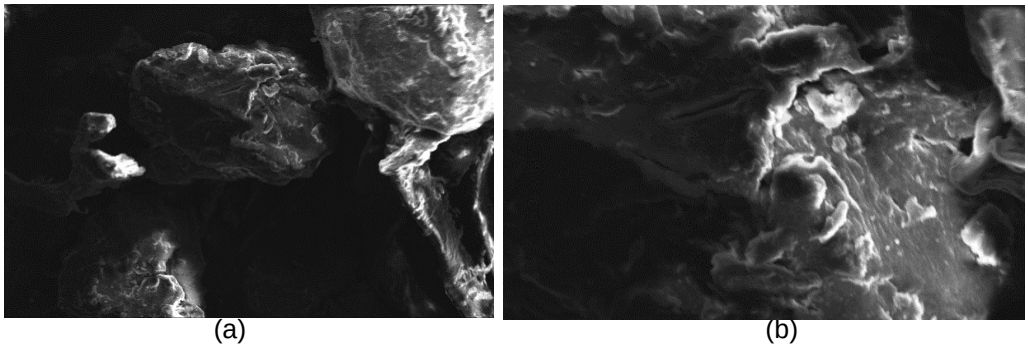

(a) (b)

**Figure 4.** SEM Results of CS/Sc composite (4:5) (a) magnification 500 X (b) magnification 1500 X

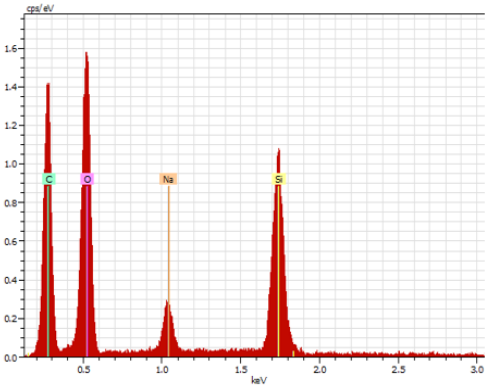


| Element | AN | Norm C (Wt %) |
|---|---|---|
| O | 8 | 59.43 |
| Si | 14 | 34.07 |
| Na | 11 | 6.5 |
| C | 6 | 0.00 |

(a)

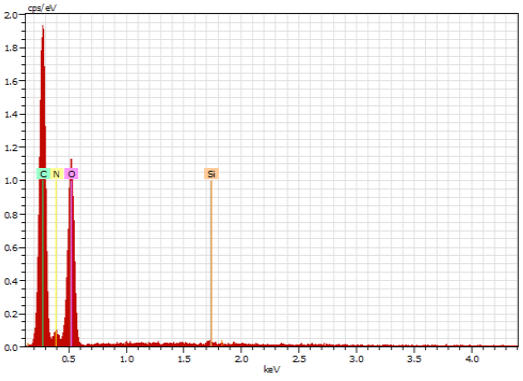


| Element | AN | Norm C (Wt %) |
|---|---|---|
| O | 8 | 91.45 |
| N | 7 | 7.80 |
| Si | 14 | 0.74 |
| C | 6 | 0.00 |

(b)

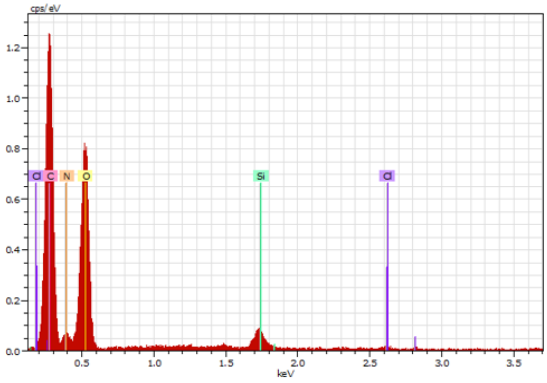


| Element | AN | Norm C (Wt %) |
|---|---|---|
| O | 8 | 84.52 |
| N | 7 | 8.46 |
| Si | 14 | 6.66 |
| Cl | 17 | 0.36 |
| C | 6 | 0.00 |

(c)

**Figure 5.** Composite EDX results CS/Sc 4:3 (a) CS/Sc 4:4 (b) CS/Sc 4:5 (c)

Elemental analysis by SEM EDX also supports these trends (Figure 5). The CS/Sc (4:3) composite contains Na, which likely originates from the silica precursor (sodium metasilicate, Na2SiO3), and Si strongly dominates the analyzed area while N from chitosan is not detected (Figure 5a). This suggests that silica aggregation may occur at this ratio, limiting the integration of chitosan within the composite. Such silica

agglomeration can reduce available surface area and weaken adsorption performance [41], which is consistent with the low q value observed for this sample (Figure 6). In contrast, the CS/Sc (4:4) and CS/Sc (4:5) composites show detectable N along with Si (Figures 5b and 5c), indicating better incorporation of chitosan within the silica network. The simultaneous presence of higher Si content and measurable N suggests improved chitosan-silica integration, which likely contributes to the higher adsorption capacity achieved at the 4:5 ratio (Figure 7).

## 4. Application of CS/Sc Composites as Fe(III) Adsorbent

The Fe(III) calibration curve is needed to determine the concentration of Fe(III) after the addition of the CS/Sc composite. The resulting calibration curve exhibits good linearity, with an $R^2$ value of 0.99793 (Figure 6). $R^2$ is the coefficient of determination, meaning that 99.79% of the concentration variable affects the absorbance [42]. The Fe(III) adsorption process using CS/Sc composite was carried out at pH two, as shown in Table 2. pH has an essential influence on the adsorption process, especially in water treatment, because pH can affect the charge of metal ions, especially Fe(III) [43]. In the adsorption process, an acidic pH is highly preferred. [44]. Application of pH 2 can prevent the precipitation of Fe(III), allowing the dissolved substance to remain in the form of positive ions ($Fe^{3+}$). Electrostatic interactions can then occur with the amine and hydroxyl groups of the composite. [43], resulting in the adsorption process.

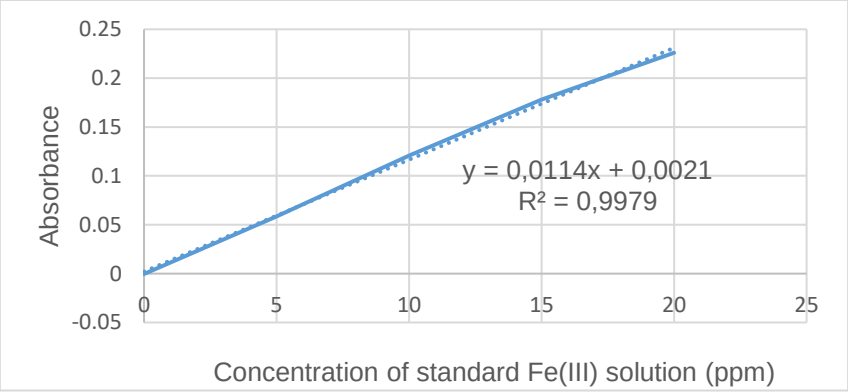


**Figure 6.** Calibration curve

**Table 2.** Adsorption of 15 ppm Fe(III) solution at pH 2 using CS/Sc composites

| Composites | Mass of composite added (gram) | Concentration of Fe(III) (ppm) | Adsorption capacity (mg/g) | Adsorption efficiency (%) |
|---|---|---|---|---|
| CS/Sc 4:3 | 0.1 | 14.218 ± 0.0087 | 0.391 | 5.211 |
| CS/Sc 4:4 | 0.1 | 9.958 ± 0.2676 | 2.701 | 36.012 |
| CS/Sc 4:5 | 0.1 | 8.469 ± 0.0182 | 3.266 | 43.542 |

Table 2 shows data on the decrease in the concentration of a 15 ppm Fe(III) solution after the addition of CS/Sc composites. The results of the analysis of

variance (ANOVA) at a significance level of 0.05 indicate that the addition of CS/Sc composite, resulting from three volume ratios, affects the decrease in Fe(III) concentration. Variations in the chitosan-silica ratio significantly affect the adsorption capacity (q) of the composite. Based on the test results, the adsorption capacity (q) increased along with the increase in the volume ratio of silica in the composite, as seen in Table 2 and Figure 7.

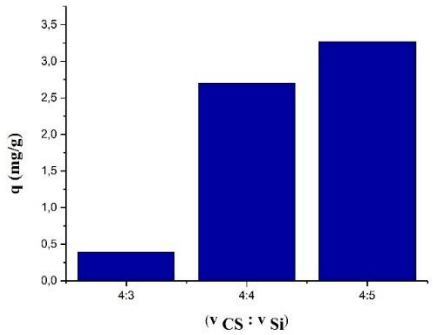


**Figure 7.** The effect of CS/Sc composite on the adsorption capacity (q) of Fe(III)

The data show that at a ratio of 4:3, the adsorption capacity (q) only reaches 0.391 mg/g, increasing to 2.701 mg/g at a ratio of 4:4, and reaching a maximum of 3.266 mg/g at a ratio of 4:5. This indicates that increasing the silica fraction in the composite significantly contributes to improving adsorption performance. The physical and chemical properties of each component can explain this increase. Chitosan, a natural polymer containing amino and hydroxyl groups, is an effective adsorbent against various contaminants, particularly heavy metal ions and polar substances [45][46][47].

However, weaknesses such as low mechanical stability [48][49], poor thermal properties, swelling in aqueous environments [47], and a limited surface area limits its adsorption capacity [49][50]. The integration of silica into the chitosan matrix overcomes these weaknesses by providing a porous structure. [51][52]. The addition of silica in the composite enhances the surface area for adsorption. [43][34] and strengthens the mechanical stability of the composite, providing more active sites for Fe(III) adsorbate interaction [53], leading to an improved adsorption capacity (q) for Fe(III) [23][43]. The silanol (Si–OH) groups on the silica surface also contribute to the formation of electrostatic interactions with the Fe(III) adsorbate, complementing the amino ($-NH_2$) and hydroxyl (-OH) groups of chitosan. [54].

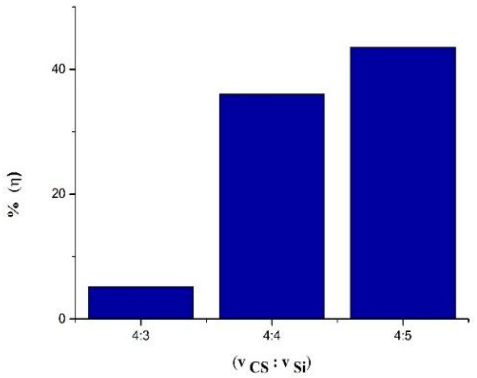


**Figure 8.** The Effect of CS/Sc composite on the adsorption efficiency (η) of Fe(III)

Figure 8 shows a trend of increasing adsorption efficiency (η) with increasing silica fraction at the CS/Sc ratio. The increase in efficiency from 5.211 % to 43.542% indicates that the addition of silica increases the total amount of adsorbate bound from the solution. This is consistent with the increase in adsorption capacity (mg/g), which reflects the amount of adsorbate successfully bound per unit mass of adsorbent.

Nevertheless, it is essential to note that increasing the proportion of silica must be optimally controlled. Although the capacity (q) and efficiency (η) increased up to a ratio of 4:5, the increase tended to slow down. The efficiency increase from 4:4 to 4:5 was only about 7.53%, compared to the significant jump from 4:3 to 4:4 of 30.80%. This indicates that at a certain ratio, the system begins to approach its optimum condition, where most of the active sites have been utilized. Furthermore, at a high silica-to-ratio, silica particles can agglomerate, reducing the availability of active sites and inhibiting the adsorbate's penetration into the matrix. [34][41].

In this context, a ratio of 4:5 appears to be the optimum point for the chitosan-silica adsorption system used in this study. Overall, increasing the silica ratio in the composite significantly enhances the adsorption efficiency, in line with previous reports that show the integration of porous inorganic materials with biopolymers can produce composite materials with excellent adsorption characteristics. [23][37][55]. The addition of silica to the chitosan matrix not only increases the adsorption capacity (mg/g) but also increases the adsorption efficiency (%) for the adsorbate.

## CONCLUSION

FTIR and SEM-EDX results indicate the successful formation of the CS/Sc composite. The composite with the best performance was produced at a ratio of 4:5 with an adsorption capacity value (q) of 3.266 mg/g and an adsorption efficiency (η) of 43.542%. The results of this study are consistent with previous research indicating that CS/Sc composites can reduce metal ion levels. The CS/Sc 4:5 composite can be further developed as a promising adsorbent for water treatment. However, this study is limited to FTIR and SEM-EDX characterization; further characterization, such as XRD, TGA, and BET, is needed to provide comprehensive results. Further research requires the addition of cross-linking agents to strengthen the structure and improve adsorption capacity.

## ACKNOWLEDGEMENT

The authors would like to thank the Institute for Lembaga Penelitian dan Pengabdian kepada Masyarakat (LPPM), Universitas Samudra, for financial support through the Penelitian Dasar Unggulan (PDU) scheme under contract number 270.93/54.6/PG/2021.

## REFERENCES

[1] M. S. Sankhla, M. Kumari, M. Nandan, R. Kumar, and P. Agrawal, “Heavy Metals Contamination in Water and their Hazardous Effect on Human Health-A Review,” *Int J Curr Microbiol Appl Sci*, vol. 5, no. 10, pp. 759–766, Oct. 2016, doi: 10.20546/ijcmas.2016.510.082.

[2] A. Odobasic, “Determination and speciation of trace heavy metals in natural water by DPASV,” in *Water Quality: Monitoring and Assessment*, Voudouris and D. Voutsa, Eds., InTechOpen, 2012, pp. 429–456. Doi: 10.5772/32339

[3] A. Valavanidis and T. Vlachogianni, “Metal pollution in ecosystems: Ecotoxicology studies and risk assessment in the marine environment,” *Sci. Adv. Environ. Chem., Toxicol., Ecotoxicol. Issues*,

2010. [Online]. Available: www.chem-tox-ecotox.org

[4] S. V. Torti and F. M. Torti, "Iron and Cancer: 2020 Vision," *Cancer Res*, vol. 80, no. 24, pp. 5435–5448, Dec. 2020, doi: 10.1158/0008-5472.CAN-20-2017.

[5] A. Singh *et al.*, "Heavy Metal Contamination of Water and Its Toxic Effect on Living Organisms," in *The Toxicity of Environmental Pollutants*, IntechOpen, 2022, pp. 1–19. doi: 10.5772/intechopen.105075.

[6] T. Wang, L. Xue, Y. Liu, T. Fang, L. Zhang, and B. Xing, "Insight into the significant contribution of intrinsic defects of carbon-based materials for the efficient removal of tetracycline antibiotics," *Chemical Engineering Journal*, vol. 435, May 2022, doi: 10.1016/j.cej.2022.134822.

[7] P. Bhatt, S. Joshi, G. M. Urper Bayram, P. Khati, and H. Simsek, "Developments and application of chitosan-based adsorbents for wastewater treatments," *Environ Res*, vol. 226, p. 115530, Jun. 2023, doi: 10.1016/j.envres.2023.115530.

[8] Y. Kong, K. Han, Y. Zhuang, and B. Shi, "Facile Synthesis of MOFs-Templated Carbon Aerogels with Enhanced Tetracycline Adsorption Performance," *Water (Basel)*, vol. 14, no. 3, p. 504, Feb. 2022, doi: 10.3390/w14030504.

[9] U. Ortiz-Ramos, R. Leyva-Ramos, E. Mendoza-Mendoza, and A. Aragón-Piña, "Removal of tetracycline from aqueous solutions by adsorption on raw Ca-bentonite. Effect of operating conditions and adsorption mechanism," *Chemical Engineering Journal*, vol. 432, p. 134428, Mar. 2022, doi: 10.1016/j.cej.2021.134428.

[10] N. Morin-Crini, M. Fourmentin, S. Fourmentin, G. Torri, and G. Crini, "Synthesis of silica materials containing cyclodextrin and their applications in wastewater treatment," *Environ Chem Lett*, vol. 17, no. 2, pp. 683–696, Jun. 2019, doi: 10.1007/s10311-018-00818-0.

[11] C. Xia *et al.*, "Adsorption of tetracycline hydrochloride on layered double hydroxide loaded carbon nanotubes and site energy distribution analysis," *Chemical Engineering Journal*, vol. 443, p. 136398, Sep. 2022, doi: 10.1016/j.cej.2022.136398.

[12] G. Gopal, S. A. Alex, N. Chandrasekaran, and A. Mukherjee, "A review on tetracycline removal from aqueous systems by advanced treatment techniques," *RSC Adv*, vol. 10, no. 45, pp. 27081–27095, 2020, doi: 10.1039/D0RA04264A.

[13] N. G. Kandile, H. T. Zaky, M. I. Mohamed, A. S. Nasr, and Y. G. Ali, "Extraction and Characterization of Chitosan from Shrimp Shells," *Open Journal of Organic Polymer Materials*, vol. 08, no. 03, pp. 33–42, 2018, doi: 10.4236/ojopm.2018.83003.

[14] W. L. Ang, A. W. Mohammad, A. Benamor, and N. Hilal, "Chitosan as natural coagulant in hybrid coagulation-nanofiltration membrane process for water treatment," *J Environ Chem Eng*, vol. 4, no. 4, pp. 4857–4862, Dec. 2016, doi: 10.1016/j.jece.2016.03.029.

[15] I. O. Saheed, W. Da Oh, and F. B. M. Suah, "Chitosan modifications for adsorption of pollutants – A review," *J Hazard Mater*, vol. 408, p. 124889, Apr. 2021, doi: 10.1016/j.jhazmat.2020.124889.

[16] M. Blachnio, T. M. Budnyak, A. Derylo-Marczewska, A. W. Marczewski, and V. A. Tertykh, "Chitosan–Silica Hybrid Composites for Removal of Sulfonated Azo Dyes from Aqueous Solutions," *Langmuir*, vol. 34, no. 6, pp. 2258–2273, Feb. 2018, doi: 10.1021/acs.langmuir.7b04076.

[17] S. Joshi and R. K. Srivastava, “Adsorptive removal of lead (Pb), copper (Cu), nickel (Ni) and mercury (Hg) ions from water using chitosan silica gel composite,” *Environ Monit Assess*, vol. 191, no. 10, p. 615, Oct. 2019, doi: 10.1007/s10661-019-7777-5.

[18] I. F. Nucifera, T. A. Zaharah, and I. Syahbanu, “Uji Stabilitas Kitosan-Kaolin Sebagai Adsorben Logam Berat Cu(Ii) Dalam Air,” *Jurnal Kimia Khatulistiwa*, vol. 5, no. 2, pp. 43–49, 2016.

[19] M. Rajiv Gandhi and S. Meenakshi, “Preparation and characterization of silica gel/chitosan composite for the removal of Cu(II) and Pb(II),” *Int J Biol Macromol*, vol. 50, no. 3, pp. 650–657, Apr. 2012, doi: 10.1016/j.ijbiomac.2012.01.012.

[20] D. Bokov *et al.*, “Nanomaterial by Sol-Gel Method: Synthesis and Application,” *Advances in Materials Science and Engineering*, vol. 2021, no. 1, Jan. 2021, doi: 10.1155/2021/5102014.

[21] M. N., B. N. Nair, and S. S., “Sodium silicate-derived aerogels: effect of processing parameters on their applications,” *RSC Adv*, vol. 11, no. 25, pp. 15301–15322, 2021, doi: 10.1039/D0RA09793D.

[22] P. M. Shewale, A. V. Rao, and A. P. Rao, “Effect of different trimethyl silylating agents on the hydrophobic and physical properties of silica aerogels,” *Appl Surf Sci*, vol. 254, no. 21, pp. 6902–6907, Aug. 2008, doi: 10.1016/j.apsusc.2008.04.109.

[23] I. Onoka and A. Hilonga, “Synthesis and characterization of aminofunctionalized chitosan-silica nanocomposite for the removal of Cu2+ from waste water,” *Discov Mater*, vol. 5, no. 1, p. 28, Feb. 2025, doi: 10.1007/s43939-025-00215-9.

[24] M. Blachnio, M. Zienkiewicz-Strzalka, A. Derylo-Marczewska, L. V. Nosach, and E. F. Voronin, “Chitosan–Silica Composites for Adsorption Application in the Treatment of Water and Wastewater from Anionic Dyes,” *Int J Mol Sci*, vol. 24, no. 14, p. 11818, Jul. 2023, doi: 10.3390/ijms241411818.

[25] M. Hudek, K. Johnston, K. Kubiak-Ossowska, V. A. Ferro, and P. A. Mulheran, “Molecular Dynamics Study of Chitosan Adsorption at a Silica Surface,” *The Journal of Physical Chemistry C*, vol. 128, no. 50, pp. 21531–21538, Dec. 2024, doi: 10.1021/acs.jpcc.4c05821.

[26] T. M. Budnyak *et al.*, “Chitosan Deposited onto Fumed Silica Surface as Sustainable Hybrid Biosorbent for Acid Orange 8 Dye Capture: Effect of Temperature in Adsorption Equilibrium and Kinetics,” *The Journal of Physical Chemistry C*, vol. 124, no. 28, pp. 15312–15323, Jul. 2020, doi: 10.1021/acs.jpcc.0c04205.

[27] D. Wang *et al.*, “Highly flexible silica/chitosan hybrid scaffolds with oriented pores for tissue regeneration,” *J Mater Chem B*, vol. 3, no. 38, pp. 7560–7576, 2015, doi: 10.1039/C5TB00767D.

[28] L. S. Connell *et al.*, “Chemical characterisation and fabrication of chitosan–silica hybrid scaffolds with 3-glycidoxypropyl trimethoxysilane,” *J. Mater. Chem. B*, vol. 2, no. 6, pp. 668–680, 2014, doi: 10.1039/C3TB21507E.

[29] M. V. Reyes-Peces *et al.*, “Chitosan-GPTMS-Silica Hybrid Mesoporous Aerogels for Bone Tissue Engineering,” *Polymers (Basel)*, vol. 12, no. 11, p. 2723, Nov. 2020, doi: 10.3390/polym12112723.

[30] Y. Amri, R. Fajri, Fitriani, P. Novitasari, and M. Zulfajri, “The Effect of Tripolyphosphate (TPP) Volumes on the Synthesis of Chitosan

Nanoparticles Using Ionic Gelation Method," 2021. doi: 10.2991/assehr.k.210909.048.

[31] G. Jozanikohan and M. N. Abarghooei, "The Fourier transform infrared spectroscopy (FTIR) analysis for the clay mineralogy studies in a clastic reservoir," *J Pet Explor Prod Technol*, vol. 12, no. 8, pp. 2093–2106, Aug. 2022, doi: 10.1007/s13202-021-01449-y.

[32] M. Olvianas, A. Widiyatmoko, and H. T. B. M. Petrus, "IR spectral similarity studies of geothermal silica-bentonite based geopolymer," 2017, p. 020015. doi: 10.1063/1.5003498.

[33] H. Liu, H. Kaya, Y. Lin, A. Ogrinc, and S. H. Kim, "Vibrational spectroscopy analysis of silica and silicate glass networks," *Journal of the American Ceramic Society*, vol. 105, no. 4, pp. 2355–2384, Apr. 2022, doi: 10.1111/jace.18206.

[34] A. Tshikovhi, S. B. Mishra, A. K. Mishra, and T. E. Motaung, "Effect of Silica Content in a Bio-Polymeric Blended Nanocomposite for Efficient Adsorption of Mercury in Basic Aqueous Solution," *Fibers and Polymers*, vol. 26, no. 2, pp. 521–535, Feb. 2025, doi: 10.1007/s12221-025-00854-y.

[35] A. Pérez-Moreno *et al.*, "Chitosan-Silica Hybrid Biomaterials for Bone Tissue Engineering: A Comparative Study of Xerogels and Aerogels," *Gels*, vol. 9, no. 5, p. 383, May 2023, doi: 10.3390/gels9050383.

[36] N. Niu, S.-H. Teng, H.-J. Zhou, and H.-S. Qian, "Synthesis, Characterization, and In Vitro Drug Delivery of Chitosan-Silica Hybrid Microspheres for Bone Tissue Engineering," *J Nanomater*, vol. 2019, pp. 1–7, Aug. 2019, doi: 10.1155/2019/7425787.

[37] P. Grzybek, Ł. Jakubski, and G. Dudek, "Neat Chitosan Porous Materials: A Review of Preparation, Structure Characterization and Application," *Int J Mol Sci*, vol. 23, no. 17, p. 9932, Sep. 2022, doi: 10.3390/ijms23179932.

[38] L. Ren, J. Xu, Y. Zhang, J. Zhou, D. Chen, and Z. Chang, "Preparation and characterization of porous chitosan microspheres and adsorption performance for hexavalent chromium," *Int J Biol Macromol*, vol. 135, pp. 898–906, Aug. 2019, doi: 10.1016/j.ijbiomac.2019.06.007.

[39] M. Chen, H. Zhao, H. Fang, and Y. Zhang, "Cross-Sectional Information on Pore Structure and Element Distribution of Sediment Particles by SEM and EDS," *Scanning*, vol. 2017, pp. 1–7, 2017, doi: 10.1155/2017/9876935.

[40] Y. Niu, W. Yu, S. Yang, and Q. Wan, "Understanding the relationship between pore size, surface charge density, and Cu2+ adsorption in mesoporous silica," *Sci Rep*, vol. 14, no. 1, p. 13521, Jun. 2024, doi: 10.1038/s41598-024-64337-5.

[41] T. Zhong, M. Xia, Z. Yao, and C. Han, "Chitosan/Silica Nanocomposite Preparation from Shrimp Shell and Its Adsorption Performance for Methylene Blue," *Sustainability*, vol. 15, no. 1, p. 47, Dec. 2022, doi: 10.3390/su15010047.

[42] N. S. L. Silalahi, Y. Amri, and P. Wahyuningsih, "Analisis Kuantitatif Logam Berat dalam Tiram (Crassostrea Sp.) dari Pesisir Kuala Langsa," *Jurnal Jeumpa*, vol. 9, no. 2, pp. 784–794, Nov. 2022, doi: 10.33059/jj.v9i2.6475.

[43] J. R. de Mello *et al.*, "Synthesis, characterization and application of new adsorbent composites based on sol-gel/chitosan for the removal of soluble substance in water," *Heliyon*, vol. 8, no. 5, p. e09444, May 2022,

doi: 10.1016/j.heliyon.2022.e09444.

[44] M.-X. Huo, Y.-L. Jin, Z.-F. Sun, F. Ren, L. Pei, and P.-G. Ren, "Facile synthesis of chitosan-based acid-resistant composite films for efficient selective adsorption properties towards anionic dyes," *Carbohydr Polym*, vol. 254, p. 117473, Feb. 2021, doi: 10.1016/j.carbpol.2020.117473.

[45] L. Zhang, Y. Zeng, and Z. Cheng, "Removal of heavy metal ions using chitosan and modified chitosan: A review," *J Mol Liq*, vol. 214, pp. 175–191, Feb. 2016, doi: 10.1016/j.molliq.2015.12.013.

[46] Y. Amri, R. Fajri, and M. S. Batu, "Chitosan Isolation and Its Application to Reduce the Content of Metal Ions in Wellbore Water,," *Jurnal Neutrino*, vol. 12, no. 1, p. 30, Jan. 2020, doi: 10.18860/neu.v12i1.8186.

[47] J. O. Gonçalves, M. M. Strieder, L. F. O. Silva, G. S. dos Reis, and G. L. Dotto, "Advanced technologies in water treatment: Chitosan and its modifications as effective agents in the adsorption of contaminants," *Int J Biol Macromol*, vol. 270, p. 132307, Jun. 2024, doi: 10.1016/j.ijbiomac.2024.132307.

[48] Y. Dago-Serry, K. N. Maroulas, A. K. Tolkou, N. C. Kokkinos, and G. Z. Kyzas, "How the chitosan structure can affect the adsorption of pharmaceuticals from wastewaters: An overview," *Carbohydrate Polymer Technologies and Applications*, vol. 7, p. 100466, Jun. 2024, doi: 10.1016/j.carpta.2024.100466.

[49] F. da Silva Bruckmann, J. O. Gonçalves, L. F. O. Silva, M. L. S. Oliveira, G. L. Dotto, and C. R. B. Rhoden, "Chitosan-based adsorbents for wastewater treatment: A comprehensive review," *Int J Biol Macromol*, vol. 309, p. 143173, May 2025, doi: 10.1016/j.ijbiomac.2025.143173.

[50] N. P. Simelane, J. K. O. Asante, P. P. Ndibewu, A. S. Mramba, and L. L. Sibali, "Biopolymer composites for removal of toxic organic compounds in pharmaceutical effluents – a review," *Carbohydrate Polymer Technologies and Applications*, vol. 4, p. 100239, Dec. 2022, doi: 10.1016/j.carpta.2022.100239.

[51] M. R. Abukhadra, M. H. Eid, M. A. El-Meligy, M. Sharaf, and A. T. Soliman, "Insight into chitosan/mesoporous silica nanocomposites as eco-friendly adsorbent for enhanced retention of U (VI) and Sr (II) from aqueous solutions and real water," *Int J Biol Macromol*, vol. 173, pp. 435–444, Mar. 2021, doi: 10.1016/j.ijbiomac.2021.01.136.

[52] J. P. Vareda, P. M. C. Matias, J. A. Paixão, D. Murtinho, A. J. M. Valente, and L. Durães, "Chitosan–Silica Composite Aerogel for the Adsorption of Cupric Ions," *Gels*, vol. 10, no. 3, p. 192, Mar. 2024, doi: 10.3390/gels10030192.

[53] H. Alkhaldi *et al.*, "Sustainable polymeric adsorbents for adsorption-based water remediation and pathogen deactivation: a review," *RSC Adv*, vol. 14, no. 45, pp. 33143–33190, 2024, doi: 10.1039/D4RA05269B.

[54] J. Liu *et al.*, "A biomimetic SiO2@chitosan composite as highly-efficient adsorbent for removing heavy metal ions in drinking water," *Chemosphere*, vol. 214, pp. 738–742, Jan. 2019, doi: 10.1016/j.chemosphere.2018.09.172.

[55] N. S. Tadayoni, M. Dinari, A. Roy, and M. Karimi Abdolmaleki, "Recent Advances in Porous Bio-Polymer Composites for the Remediation of Organic Pollutants," *Polymers (Basel)*, vol. 16, no. 11, p. 1543, May 2024, doi: 10.3390/polym16111543.